Overview

Study area

EMI survey and inversion

Soil sampling and analysis

Site-specific calibration

Soil salinity and sodicity mapping

Discussion Conclusion

Evaluation of soil salinity and sodicity using electromagnetic conductivity imaging

M Farzamian[1,2], F.J Martinez-Moreno[2], T.B Ramos[3], N Castanheira[1], A.M Paz[1], F.A Monteiro Santos[2], C.A Alexandre[4], M.C Paz[2,5], M.R Rodríguez[6], K Vanderlinden[6], and M.C Gonçalves[1]

[1]INIAV, Instituto Nacional de Investigação Agrária e Veterinária, Oeiras, Portugal, (mohammadfarzamian@gmail.com)
[2]Instituto Dom Luiz (IDL), Faculdade de Ciências, Universidade de Lisboa, Campo Grande, 1749–016, Lisboa, Portugal
[3] Universidade de Lisboa, Instituto Superior Técnico, Lisboa, Portugal
[4] Universidade de Évora, institute of Mediterranean Agricultural and Environmental Sciences, Évora, Portugal,
[5] CIQuiBio, Barreiro School of Technology, Polytechnic Institute of Setúbal, Rua Américo da Silva Marinho, 2839-001 Lavradio, Portugal
[6] IFAPA Centro Alameda del Obispo, Córdoba, Spain

PICO Navigation

You are invited to click on the different sections outlined on this slide to obtain more information on that particular section. Clicking the ✖ on top left of a slide will always bring you back to the first slide. This PICO will present the results of our study in an important agricultural region near Lisbon, Lezíria Grande, with very high biological, agronomic and socio-economical value. For more information about this PICO please see our work, published in Geoderma.

Paz, A., Castanheira., N., Farzamian, M., Paz, M.C., Gonçalves, M., Monteiro Santos, F., and Triantafilis, J. 2020. Prediction of soil salinity and sodicity using electromagnetic conductivity imaging. **Geoderma**, 361, 114086, [https://doi.org/10.1016/j.geoderma.2019.114086.](https://doi.org/10.1016/j.geoderma.2019.114086)

Overview

Soil salinity problems can refer to an excess of soluble salts (saline soils), a dominance of exchangeable sodium in the soil exchange complex (sodic soils), or a mixture of both situations (saline-sodic soils). In saline soils, the large osmotic pressure of the soil solution makes it difficult for plants to absorb enough water. Nutritional imbalances or toxicity caused by specific ions can also arise. Even tough, saline soils can generally maintain their porosity and permeability, with excess of soluble salts capable of being leached with low conductivity water and so long as there is sufficient drainage. Sodic soils have an excess of exchangeable Na and low concentration of soluble salts, which leads to the swelling and dispersion of the soil particles in the soil solution and to the formation of layers with low permeability, which among other drawbacks, restricts root growth and enhances soil erosion. Saline-sodic soils have both excess of soluble salts and of exchangeable Na. In this case, the high concentration of dissolved salts is able to counteract the particles dispersion, however if the soluble salts are leached, the degradation of the soil structure occurs with consequent changes in the soil porosity and permeability. These categories are important because the adverse consequences and management vary accordingly.

The determination of these categories require invasive soil sampling and time-consuming laboratory analysis, given the large number of soil samples that need to be collected to characterize the soil salinization. To improve soil surveying efficiency, geophysical techniques such as electromagnetic induction (EMI), have been applied for soil characterization, as they allow for rapid, repeatable and accurate, non-invasive analysis, covering large areas in a short time and at relative low cost. EMI measures the apparent electrical conductivity of the soil (EC_a), which is affected by soil properties such as salinity, water content, and the soil's particle size distribution. EC_a data can be then inverted using mathematical methods to generate electromagnetic conductivity images (EMCI), which provide the vertical distribution of the soil electrical conductivity (σ). σ can be converted to soil salinity and sodicity indicators such as electrical conductivity of the soil saturation paste extract (ECe), sodium adsorption ratio (SAR), and exchangeable sodium percentage (ESP) by determining whether a relationship can be established, and which usually depends on location-specific condition.

EMI method

EM sensors consist of two coils: the first one is the transmitter, which is energized with an alternating current at a specific frequency; the second one, located at a short distance, is the receiver. The variable magnetic field created by the transmitter (the primary field) induces electrical currents in the subsurface. These currents generate a secondary magnetic field, which is detected, together with the primary field, by the receiver coil. The investigation depth depends on the frequency of the energizing field, on the electrical structure of the earth and also on the intercoil spacing and coil configuration (vertical dipole or horizontal dipole mode). In the vertical dipole mode (VMD), the transmitter and receiver coils are located horizontally while in the horizontal dipole mode (HMD) these are placed vertically on the ground surface. The use of different intercoil spacing and operating modes allows us to construct an image of the subsurface electrical conductivity distribution.

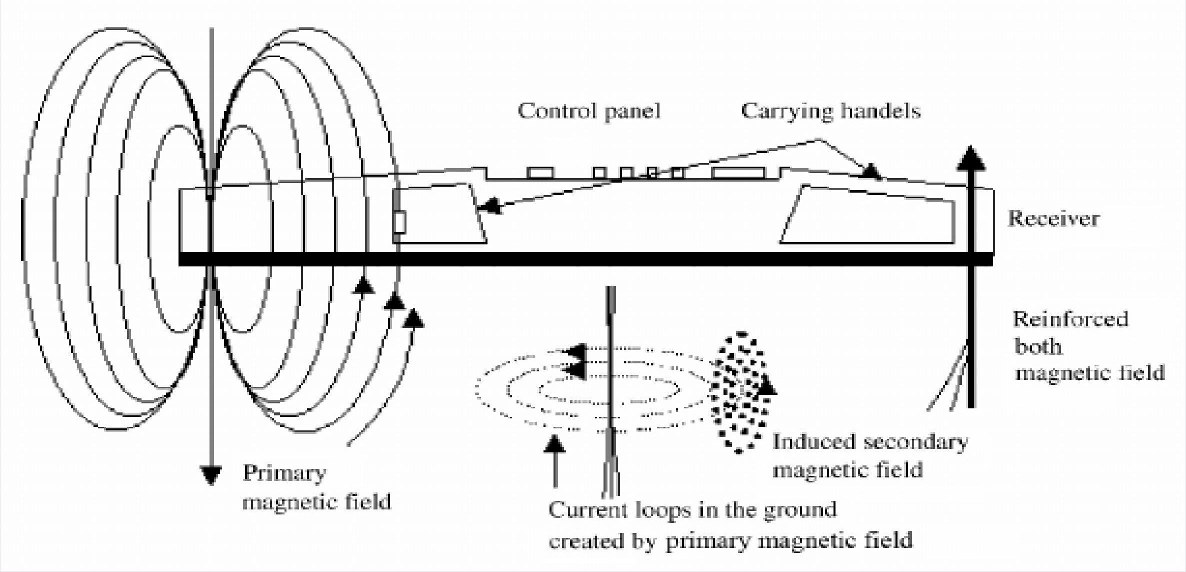

Overview

Data inversion

To invert EC_a data, we used EM4SOIL software to generate EMCIs. The 1D laterally constrained method (Monteiro Santos, 2004) has been modified in this software to invert EC_a data, where each 1D conductivity model, obtained beneath each measurement site, is constrained by its neighbors. The earth model used in the 2D forward model consists of a mesh of a number of blocks distributed according to the locations of the measurement sites and coil spacing. Two forward modeling subroutines, one based on the cumulative response (McNeill, 1980) and another based on the full solution of the Maxwell equations (Kaufman and Keller, 1983) are used in this software allowing the use of the algorithm in regions characterized by high-conductivity contrast. The damping factor in this program is a Lagrange multiplier and is used to control the balance between data fit and the smoothness difference of the model from the a priori model.

References:
Monteiro Santos, F.A. 2004. 1-D laterally constrained inversion of EM34 profiling data. J. Appl. Geophys. 56:123–134.
McNeill, J.D., 1980. Electromagnetic terrain conductivity measurement at low induction numbers. Geonics Limited, Technical Note TN-6.
Kaufman, A.A., and G.V. Keller. 1983. Frequency and transient soundings. Methods in Geochem. and Geophys. 16. Elsevier, New York.

Study area

The study area in Portugal is located in Lezíria Grande, Vila Franca de Xira, northeast of Lisbon, which is a 13.000 ha irrigated area, 1 to 2 m above sea level and flanked by rivers Tejo and Sorraia. The region is at risk of salinisation due to its proximity to the Tagus River estuary and the influence of estuarine tides on groundwater, inducing waterlogging and soil salinization problems.

Four study sites were selected, along a north-side direction, in order to cover some of the known variance in the area, as shown in the Figure. Soils are typically clayey and homogeneous with fine to very fine texture.

- **Crops**: Tomato (1), maize (d and 3), pasture (4)

- **Rainfall** 827 mm/y
- **ETP** 911 mm/y
- **Average temperature** 16.5°C
- **Minimum temperatute** 1.7°C
- **Maximum temperature** 40.7 °C

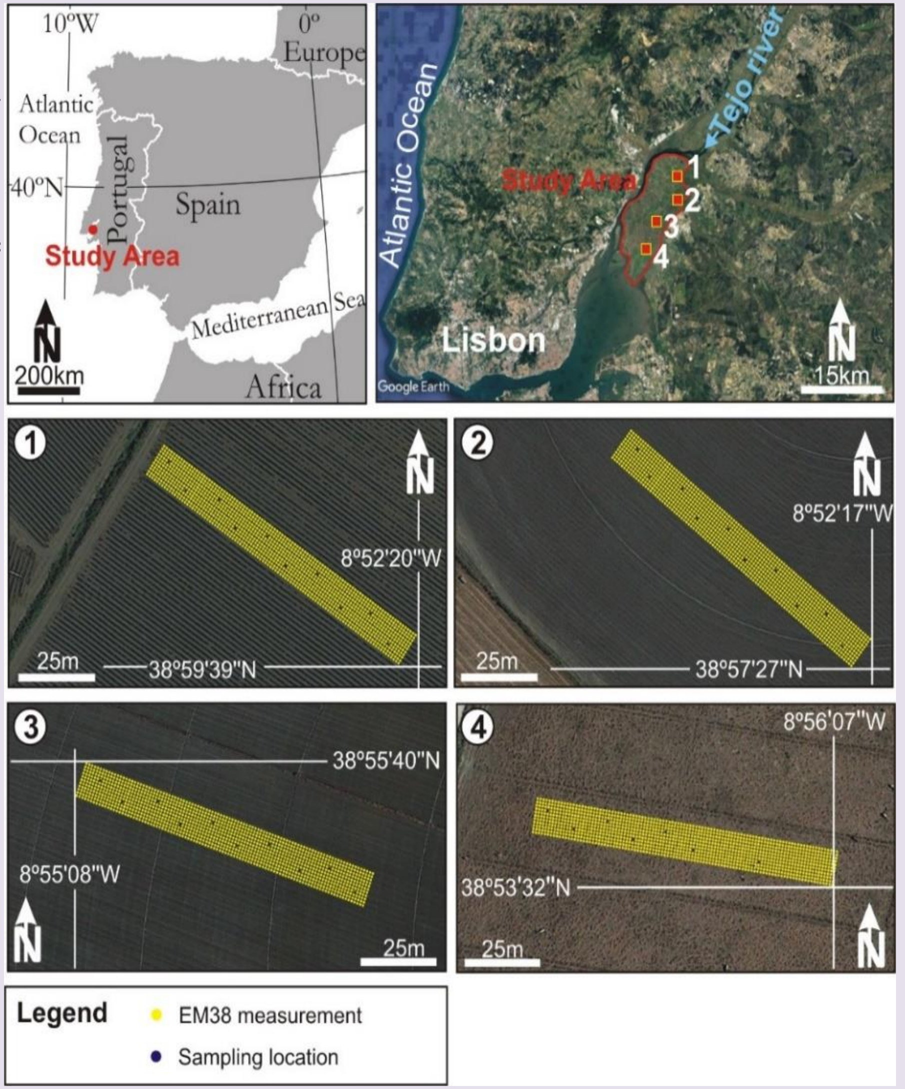

EMI survey and inversion

EMI survey

At each of the four locations, EMI measurements were collected during the months of May and June 2017, along 100 m long transects, using the EM38 (Geonics Ltd, Mississauga, Canada). Because the EM38 is a single-coil instrument, it measures EC_a only at a single mode in each pass. Therefore, EC_a was collected in the horizontal (EC_{ah}) and vertical (EC_{av}) orientations and at two heights. This provides an insight to soil electrical conductivity change with depth. The first measurement pair was made at the height from the soil surface of 0.15 m, which allows a theoretical depth of measurement of 0.6 m ($EC_{ah0.15}$) and 1.35 m ($EC_{av0.15}$). The second measurement pair was made at a height of 0.4 m, which allows a theoretical depth of measurement of 0.35 m ($EC_{ah0.4}$) and 1.1 m ($EC_{av0.4}$). EC_a data was collected continuously, using a cart that enabled the position of the EM38 instrument in the four modes, using a GPS (Rikaline 6010) for registration of the position.

EMI inversion

All EC_a data, collected at the four locations, were inverted by applying a five-layer earth initial model with electrical conductivity of 100 mS m^{-1} and a fixed layer thickness of 0.3 m to estimate σ at the following layers where we collected soil samples: topsoil (0-0.3 m), subsurface (0.3-0.6 m), upper subsoil (0.6-0.9 m), intermediate subsoil (0.9-1.2 m), and lower subsoil (1.2-1.5 m). To run the algorithm, several parameters were tested and selected, such as the type of inversion algorithm, the number of iterations, and the smoothing factor (λ) that controls the roughness of the model.

EMI survey and inversion

EMI data (Selected transect at each location)

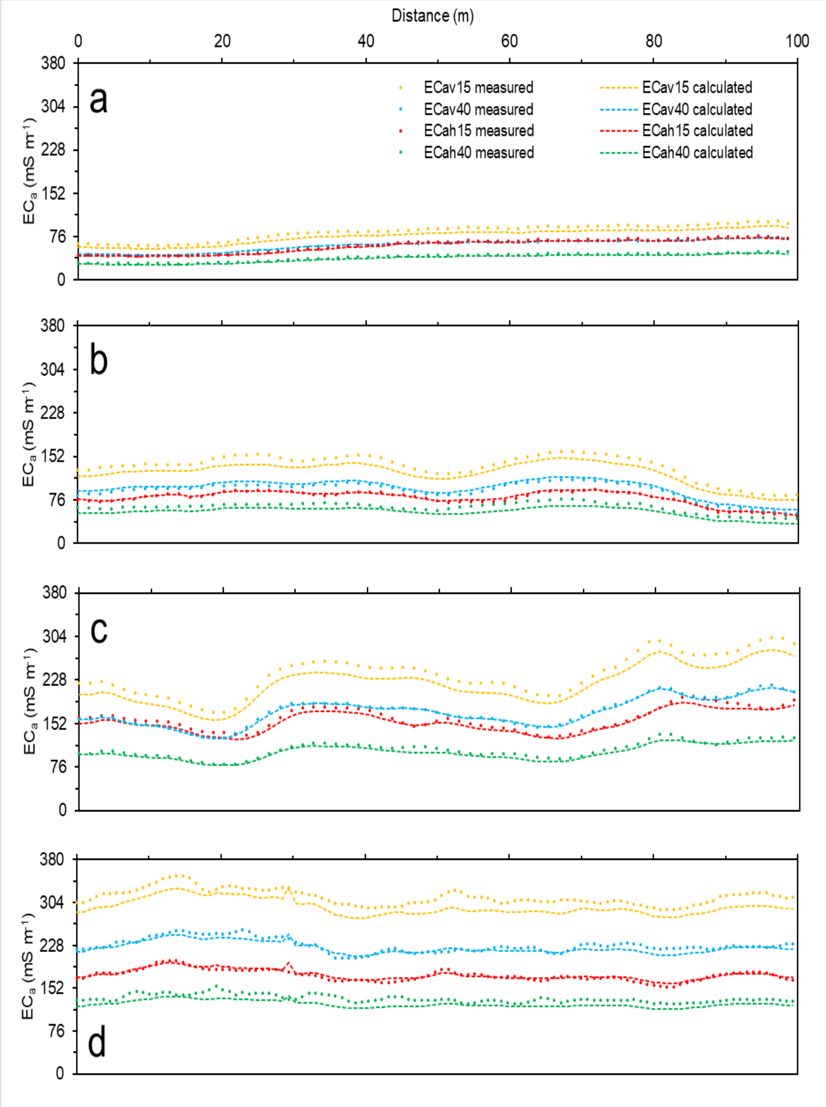

EC_a across location 1 (a) is generally small, with all four measured EC_a less than 70 mS/m. Of all the measurements, the $EC_{ah0.4}$ data were smallest, with $EC_{ah0.15}$ and $EC_{av0.4}$ similar and $EC_{av0.15}$ largest.

EC_a across location 2 (b) is generally twice as large compared to location 1. In addition, EC_{av} was generally twice as large as EC_{ah} at either height.

EC_a across location 3 (c) increases again by a factor of two. As with the other two transects, EC_a was smallest for the $EC_{ah0.40}$ with $EC_{av0.4}$ next, followed closely by $EC_{ah0.15}$ with $EC_{av0.15}$ again largest. EC_a oscillates most along this transect, showing the greatest variation

EC_a across the location 4 (d) is clearly largest. The EC_{ah} is smaller than EC_{av} along all transects suggest topsoil and subsurface conductivity would, in principle, be smaller than that in the subsoil.

EMCI the vertical distribution of σ

EMI survey and inversion

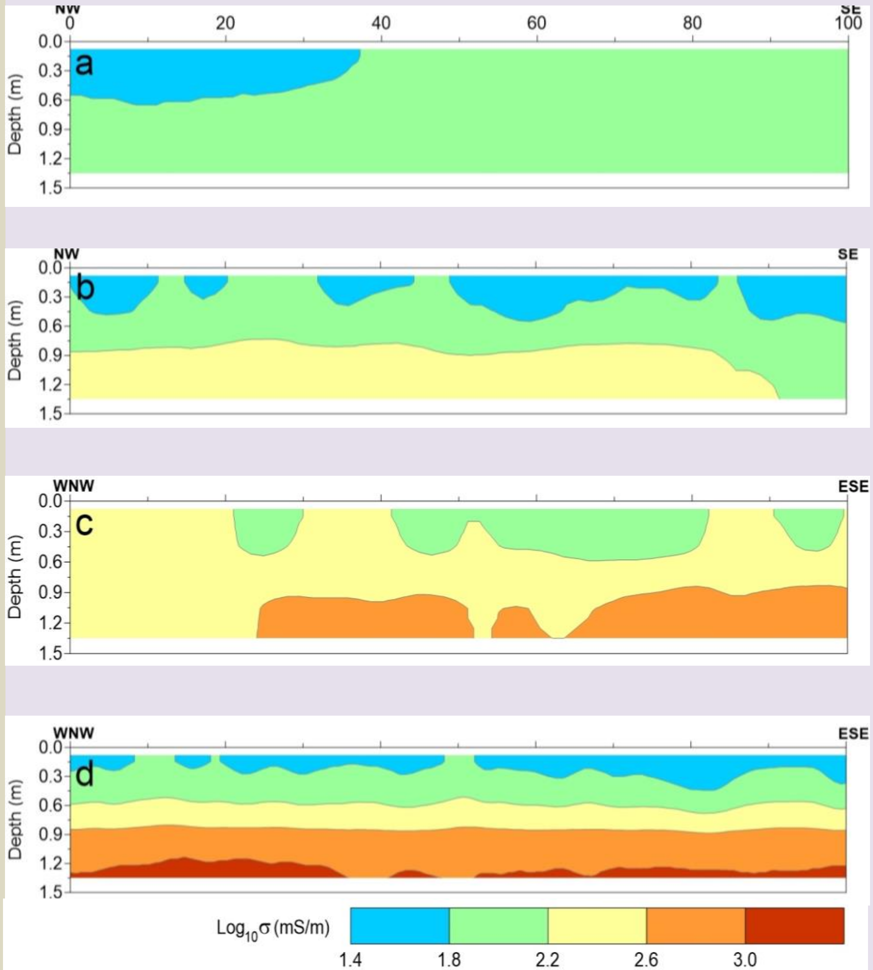

EMCIs were obtained through the inversion of $EC_{ah0.15}$, $EC_{av0.15}$, $EC_{ah0.40}$, and $EC_{av0.40}$ data using the optimal parameters, described in Farzamian et al. 2019.

The calculated model responses of the shown EMCIs are presented in the dashed lines in the pervious Figure. For all locations, there is a good agreement between the model responses and the measured EC_a, which indicates reliable EMCIs.

Globally, *σ* ranges from about 20 to 1500 mS m^{-1}, with the lowest values at location 1 and the highest at location 4. A general increasing trend of *σ* is quite evident from the north to the south, accompanying the previously known soil salinity gradient. In addition, *σ* increases with depth at locations 2, 3, and 4. At location 1, *σ* ranges spatiotemporally from 20 to 130 mS m^{-1}. At location 2, *σ* ranges from 30 to 500 mS m^{-1}, with the highest values at depth. A similar pattern of *σ* is evident at locations 3 and 4. However, a greater range of *σ* is seen at location 3, with values from 50 to 700 mS m^{-1}. Location 4 exhibits the largest variations of *σ*, ranging from 40 to 1500 mS m^{-1}.

Farzamian, M., Paz, M.C., Monteiro Santos, F., Gonçalves, M.C., Paz, A.M., Castanheira., N.L., Triantafilis, J. 2019. Mapping soil salinity using electromagnetic conductivity imaging – a comparison of regional and location-specific calibrations. **Land Degradation and Development** 30, 1393–1406. https://doi.org/10.1002/ldr.3317

Soil sampling and Labratory analysis

Soil samples were collected at five layers to a depth of 1.35 m, at sampling sites along the EMI transects, and used for laboratory determination of the soil physico-chemical properties – electrical conductivity of the soil saturation paste extract (EC_e), sodium adsorption ratio (SAR), pH, cation exchange capacity (CEC), exchangeable sodium percentage (ESP), volumetric water content (θ), and particle size distribution. EC_e, SAR, and pH are measures of ions present in the soil solution, and CEC and ESP are measures of the ions adsorbed at the soil solids.

EC_e was determined with a conductivity meter (WTW 1C20-0211 inoLab) in the extract collected with suction filters from the soil saturation paste. SAR is a measure of the dominance of soluble Na relatively to the concentrations of soluble Ca and Mg and is measured in the soil saturation paste extract, through atomic absorption spectrometry (Thermo Scientific iCE3000). ESP is a measure of the dominance of Na in the exchange complex. ESP is determined as the ratio between the exchangeable Na obtained with the Bascomb method and CEC, and is expressed as a percentage.

The classification presented in Table below was used as a base to classify the soils according to salinity and sodicity.

Soil classification	EC_e	SAR	ESP	pH
	dS m^{-1}	(mEq $L^{-1})^{0.5}$	%	
Non-saline and non-sodic	< 4	< 13	< 15	< 8.5
Saline-sodic	≥ 4	≥ 13	≥ 15	≤ 8.5
Saline	≥ 4	< 13	< 15	< 8.5
Sodic	<4	≥ 13	≥ 15	> 8.5

For more info please see:

Paz, A., Castanheira., N., Farzamian, M., Paz, M.C., Gonçalves, M., Monteiro Santos, F., and Triantafilis, J. 2020. Prediction of soil salinity and sodicity using electromagnetic conductivity imaging. **Geoderma**, 361, 114086, https://doi.org/10.1016/j.geoderma.2019.114086.

Soil physico-chemical properties

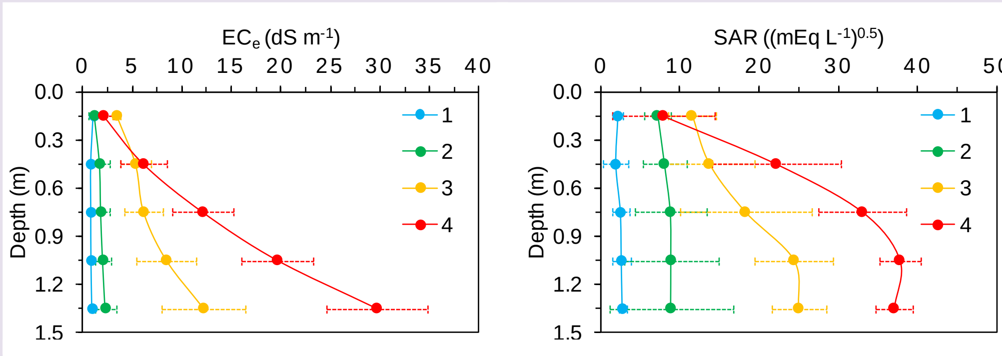

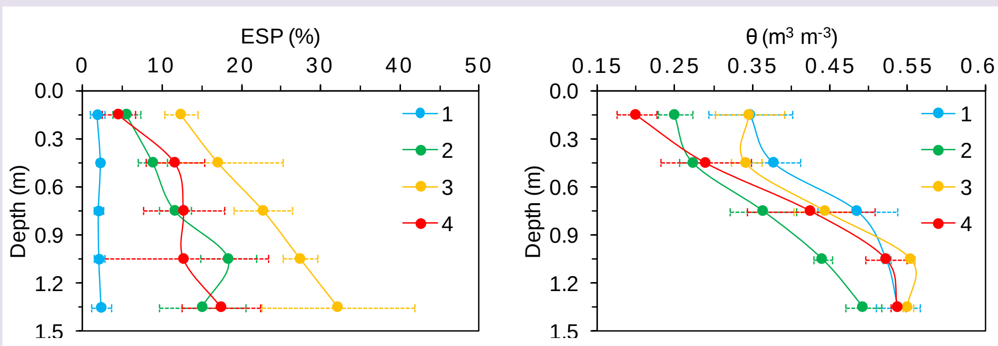

Locations 1 and 2 were uniformly non-saline, with EC_e below 2 dS m^{-1}. At location 3, the mean of EC_e increases markedly with depth from non-saline (<4 dS m^{-1}) in the topsoil to 12 dS m^{-1} in the lower subsoil. At location 4, EC_e was also non-saline in the topsoil increasing to 30 dS m^{-1} in the lower subsoil.

The mean of SAR follows a trend similar to that of EC_e, considering the variation between locations and with depth at each location. At locations 1 and 2, SAR is generally below 13 (mEq $L^{-1})^{0.5}$ along the entire profile (non-sodic soil). At locations 3 and 4, SAR exceeded 13 (mEq $L^{-1})^{0.5}$ in layers below the subsurface,

ESP showed an increment with depth at locations 2, 3, and 4, but location 3 evidenced the maximum values for ESP. At location 1, the mean values of ESP were always below 15% (non-sodic soil). At the subsurface and subsoil at location 3 and at some subsoil layers at locations 2 and 4, ESP is over 15%.

Considering θ, its mean value increased consistently with depth at all locations.

Soil sampling and analysis

Soil physico-chemical properties

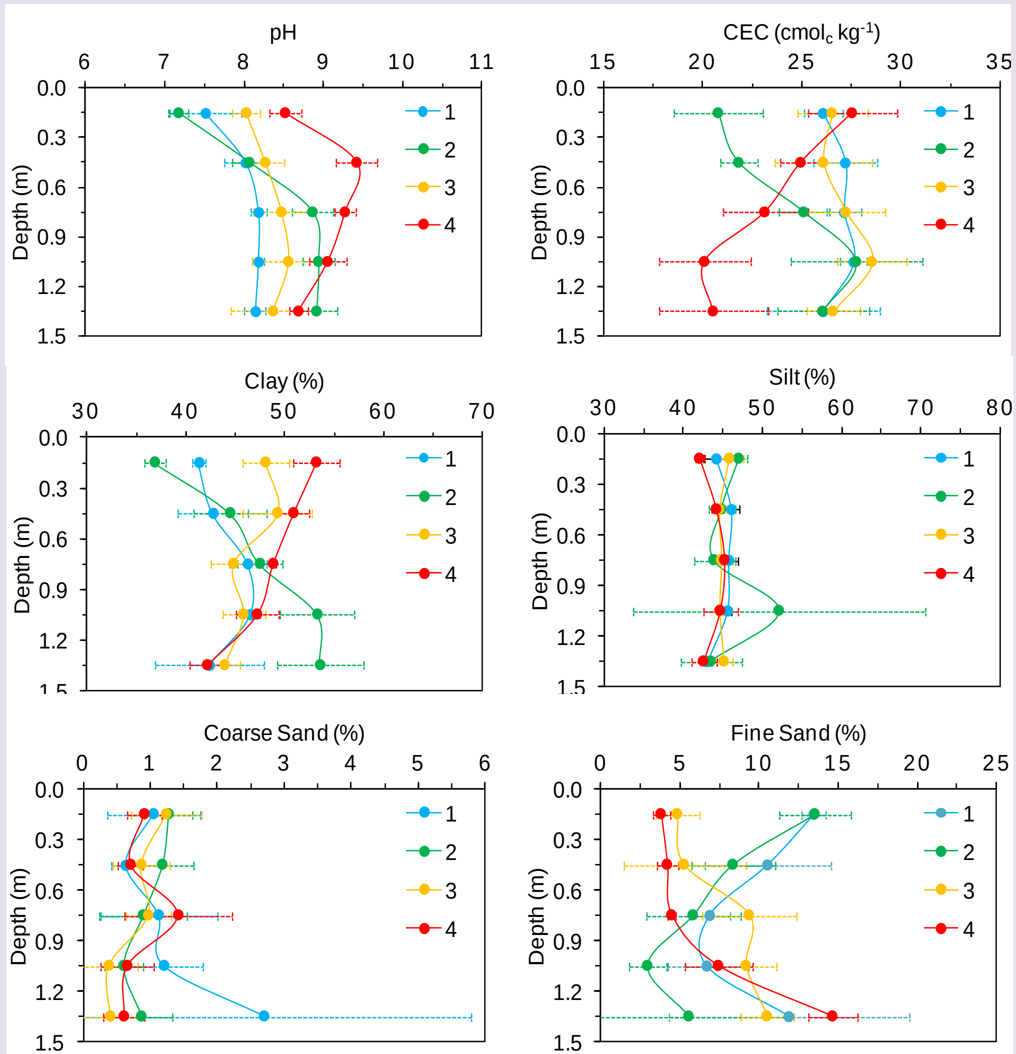

The mean of soil pH generally increased from the topsoil to the subsurface layers and showed relatively uniform mean values in the subsoil layers at locations 1, 2, and 3, with a small decrease with depth at location 4. The mean values of soil pH were generally over 8.5 (typical of sodic soils) at location 4 and subsoil layers at location 2. The mean values of CEC are relatively uniform with depth at locations 1 and 3, but showed an increase with depth at location 2 and a decrease with depth at location 4. Considering θ, its mean value increased consistently with depth at all locations. Considering the particle size distribution, locations 3 and 4 had larger clay content at the topsoil and subsurface, which decrease with depth, while location 2 showed a consistent increment of clay with depth. The silt and coarse sand fractions showed relatively uniform mean values. The increase of CEC with depth for location 2 can be related to the increment of the clay fraction with depth at this location. The results also indicate that EC_e, SAR, pH, CEC, and ESP are not similarly correlated at the different locations

Sample classification according to salinity and sodicity

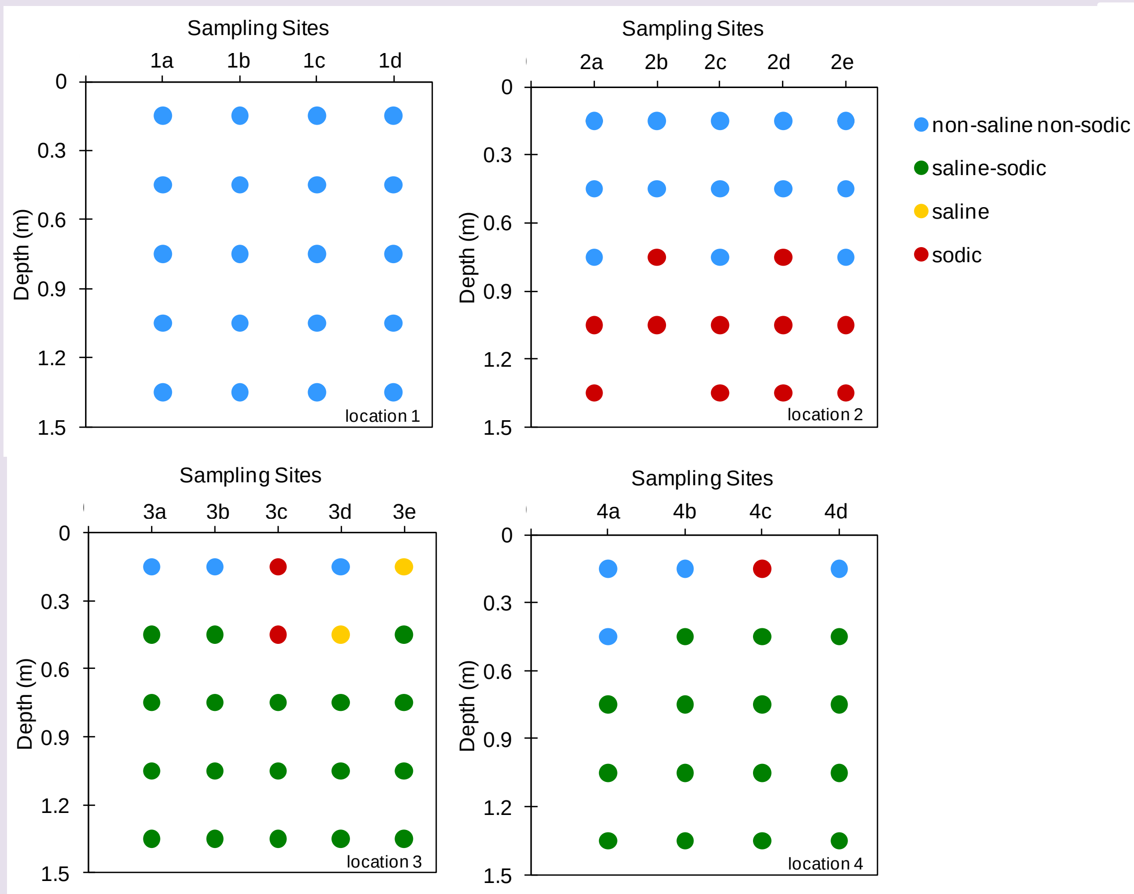

The limits for EC_e, ESP and SAR presented in the pervious Table were used to classify the soil according to salinity and sodicity. At location 1, all samples were classified as non-saline and non-sodic. At location 2, the topsoil and subsurface were also non-saline and non-sodic, which was also the case at three of the sites in the upper subsoil, while below this layer all the samples were sodic. At locations 3 and 4 the topsoil was for the most part non-saline and non-sodic, with the most of the subsurface and subsoil samples saline-sodic.

We now evaluate how well the EMI data, modelling and calibration can predict these classifications.

Soil sampling and analysis

Correlation analysis and prediction of salinity and sodicity

We analysed the ability of EMCIs for classifying the soil according to salinity and sodicity from EC_e, SAR, and ESP. Regression models were developed for prediction of EC_e, SAR and ESP and the prediction ability of the regression models was analysed through cross-validation, using the leave-one-out cross validation. In this method one sample was removed and a calibration was established based on the remaining samples to predict the value of the removed sample. This procedure was repeated for each sample in an iterative manner, until all samples were removed once. The root mean square error of the prediction (RMSEP) was calculated according to equation:

$$RMSE = \sqrt{\frac{\sum(measured - predicted)^2}{n}}$$

The regression models were then used to produce 2-D maps with the soil classification according to salinity and sodicity, obtained from the EMCI transects at each location.

Site-specific calibration

Site-specific calibration

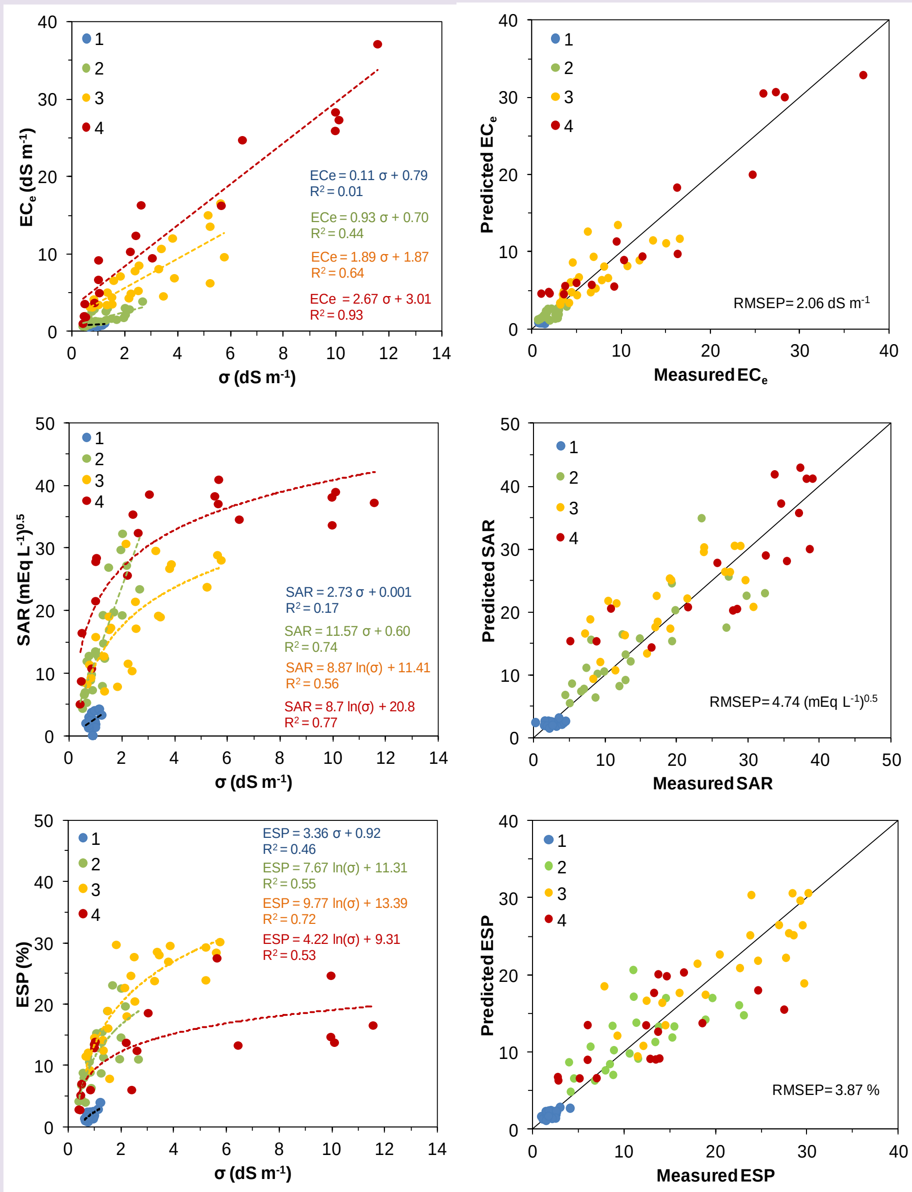

Linear regression models were well-suited for the location-specific relations between EC_e and σ.

Regression models between SAR and σ and between ESP and σ were logarithmic, except for SAR at location2.

Location 1 showed very low correlation between EC_e and σ and between SAR and σ. This was most likely because EC_e and SAR at location 1 have relatively low values and minimal variations, and σ is dominated by other properties at this location. Although, as the values of σ at location 1 were also relatively low, it is possible to predict a nom-saline and non sodic soil from σ.

The leave-one-out cross validation for all the samples at the four locations resulted in a RMSEP of 2.06 dSm^{-1} for EC_e, 4.74 $(mEq\ L^{-1})^{0.5}$ for SAR, and 3.87 % for ESP. The results indicate that it is possible to predict these variables with acceptable prediction errors within the measured range.

2-D maps of soil salinity classification

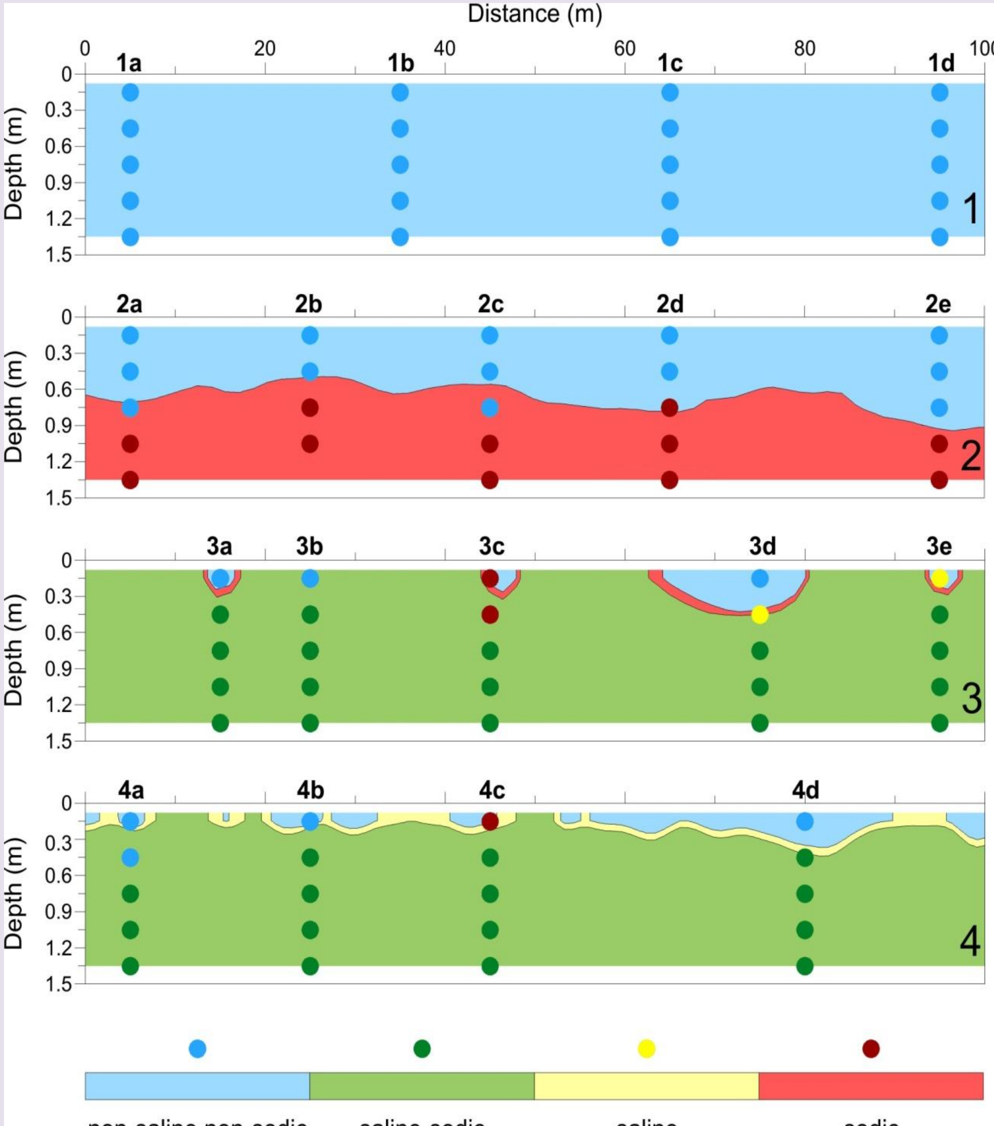

The σ obtained from EMI transects measured at the four locations was used to classify the soil according to salinity and sodicity, from the predicted EC_e, SAR and ESP. The circles represent the actual classification obtained from EC_e, SAR, and ESP measured at each sample presented in the previous Figure. There is generally good agreement between the predicted classification and the actual classification obtained from the samples, with 88.6% of the samples correctly classified. Some samples were not correctly classified mainly at the top-soil and upper. These misclassifications occur mainly in layers with a change in the classification at the neighbouring layer.

The classification error could be due to the variability within the layer, as the sample is taken at the middle depth for each layer. It could also be a result of the effects of smoothing from the regularization applied in the inversion algorithm, which can smooth the sharp changes that occur between layers. In addition, the four EC_a measurements can be insufficient for recovering sharp variability of σ with depth.

Soil salinity and sodicity mapping

Discussion and Conclusion

Inversion of multi-heights/multi-sensors data can be used to image soil electrical conductivity.

Soil electrical conductivity images can be converted to soil salinity and sodicity predictors using an in-situ site calibration when salinity is dominate factor in conductivity changes.

The EMI and soil analyses results permitted identifying important imbalances at some of the locations. At location 2, the subsoil layers were classified as sodic and therefore are facing degradation of their structure. While the root zone for irrigated maize at this location is until about 0.5 m, where samples were non-saline and non-sodic, the degradation of layers below can result in a decrease of permeability and promote salts accumulation in the root zone, and consequent productivity loss. At locations 3 and 4 the subsoil was mainly saline-sodic. The presence of salts other than Na prevents the structure degradation at these layers, but it is very important to have in consideration that the washing of the soluble salts will result in sodic layers, with the above-mentioned degradation risks. This could be an eminent risk at location 3, where the crops are irrigated and therefore the soil could be more prone to leaching of the soluble salts than location 4.

Soil salinity and sodicity management is usually large scale challenges. EM method is a non-invasive, fast and cost-effective technique that may be used for sali in regional scale.

Repeated EM data along the same transects can be used to monitor salinity and sodicity with time. However, variations of other parameters (i.e. Moisture content, groundwater level) make it difficult to assess the dynamic of soil salinity and sodicity.

We cannot use geophysical imaging alone – we need to use other data to support geophysical data.